increases, the higher order echoes disappear and only the normal $t=\tau$ echo remains.

IV. DISCUSSION

It is seen that the multiple echoes occur when the spins are strongly coupled to the resonant cavity. The general formalism applied to the quantum-mechanical harmonic oscillator should apply to other systems such as optical energy levels in an optical system.[8]

The relaxation processes of the magnons are divided into homogeneous and inhomogeneous broadening. The relaxation processes[9] which proceed via the coupling to the Maxwell field will be strongly dependent upon the mode structure imposed by the microwave cavity. Further measurements of T_1 and T_2 are in progress in this system.

ACKNOWLEDGMENT

It is a pleasure to acknowledge helpful discussions with Dr. J. Hernandez.

[8] N. A. Kurnit, I. D. Abella, and S. R. Hartmann, Phys. Rev. Letters **13**, 567 (1964); A. G. Fox and P. W. Smith, *ibid.* **18**, 826 (1967); S. L. McCall and E. L. Hahn, *ibid.* **18**, 908 (1967).

[9] M. Sparks, *Ferromagnetic Relaxation Theory*, (McGraw-Hill Book Co., Inc., New York, 1964).

PHYSICAL REVIEW VOLUME 167, NUMBER 2 10 MARCH 1968

Transition Temperature of Strong-Coupled Superconductors

W. L. McMillan
Bell Telephone Laboratories, Murray Hill, New Jersey
(Received 29 August 1967)

The superconducting transition temperature is calculated as a function of the electron-phonon and electron-electron coupling constants within the framework of the strong-coupling theory. Using this theoretical result, we find empirical values of the coupling constants and the "band-structure" density of states for a number of metals and alloys. It is noted that the electron-phonon coupling constant depends primarily on the phonon frequencies rather than on the electronic properties of the metal. Finally, using these results, one can predict a maximum superconducting transition temperature.

I. INTRODUCTION

In this paper we derive a formula for the superconducting transition temperature, using the so-called "strong-coupled" theory, as a function of the coupling constants for the electron-phonon and Coulomb interactions. We take the point of view here that the theory of superconductivity is accurate and well-developed and that, given certain properties of the normal state of a given metal, we could calculate its superconducting properties, e.g., T_c, with an accuracy $\sim 1\%$. The necessary properties of the normal state are (a) the electron energy bands near the Fermi energy, (b) the phonon dispersion curves, (c) the fully dressed (screened) electron-phonon interaction matrix elements, and (d) the fully dressed Coulomb interaction between electrons. All these properties are not sufficiently well-known for any metal to make a first-principles calculation of its superconducting properties worthwhile. There is much to be learned, however, by approaching the problem from the other direction and asking what can be learned about the normal metal from its measured superconducting properties. There are available for a number of superconducting metals and alloys measurements of the superconducting transition temperature T_c, the Debye temperature Θ, and the electronic heat-capacity coefficient γ. Also, for a few metals, there are measurements of the phonon energies and of the isotope shift of T_c. By making use of our theoretical formula for T_c and experimental data, we can find empirical values for electron-phonon coupling constant λ and the phonon enhancement of cyclotron mass and specific heat. The measured isotope shifts can be used to find empirical values for the Coulomb coupling constant μ^*. With the addition of information about the phonon energies, we will be able to examine the makeup of λ and discuss the influence of the various metallic properties upon the variations of λ throughout the periodic table. Finally, it will be pointed out that the theory makes a reasonably definite statement about the maximum T_c that one should expect for a given class of materials.

The plan of the paper is as follows. In Sec. II we will write down the integral equations for the strong-coupled superconductor at the transition temperature and discuss an approximate, analytic solution. In Sec. III we will present accurate numerical solutions of the integral equations and show that these results for T_c fit a simple analytic function of the coupling constants λ and μ^*. In Sec. IV we use these theoretical formulas and experimental data to find empirical values of λ and the "band-structure" electronic density of states at the Fermi surface for a number of metals and alloys. In Sec. V we derive an expression for λ in terms of an average phonon energy $N(0)$, and an average of the electron-phonon matrix elements, and find empirical values for these quantities for a few elements. We

present a theoretical argument and empirical evidence that the coupling constant depends strongly on the phonon energies and only weakly on the other parameters in a given class of materials. With this observation, we derive in Sec. VI a maximum T_c for that class of materials.

II. THEORY

According to the Bardeen-Cooper-Schrieffer[1] (BCS) theory of superconductivity, one has a relation between the transition temperature T_c, a typical phonon energy $\langle\omega\rangle$, and the interaction strength $N(0)V$:

$$T_c = 1.14\langle\omega\rangle \exp[-1/N(0)V]. \quad (1)$$

Here $N(0)$ is the electronic density of states at the Fermi surface and V is the pairing potential arising from the electron-phonon interaction. Numerous authors have estimated $N(0)$ and V using Eq. (1) and experimental values of T_c, Θ, and γ (the coefficient of the electronic specific heat).

Since the BCS paper, much progress has been made in understanding the role of the electron-phonon interaction in normal and superconducting metals. Migdal[2] showed that, in normal metals, the electron-phonon interaction could be treated accurately [to order $(m/M)^{1/2}$] even for strong coupling. Eliashberg[3] and Nambu[4] have extended the Migdal treatment to the superconducting state using the Green's-function techniques of Gor'kov.[5] The Eliashberg theory takes into account the retarded nature of the phonon-induced interaction and treats properly the damping of the excitations. This strong-coupling theory is also accurate to order $(m/M)^{1/2}$. With the addition of the pseudopotential treatment[6] of the screened Coulomb interaction, the Eliashberg equations represent the present state of the art in superconductivity theory.[7] Comparison with tunneling experiments[8,9] and critical-field measurements[10] for strong-coupled superconductors has provided a strong confirmation of the theory in its present form.

The integral equations for the normal and pairing self-energies at the transition temperature are[11,12]

$$\xi(\omega) = [1-Z(\omega)]\omega = \int_0^\infty d\omega' \int_0^{\omega_0} d\omega_q\, \alpha^2(\omega_q) F(\omega_q) \times\{[N(\omega_q)+f(-\omega')][(\omega'+\omega_q+\omega)^{-1}-(\omega'+\omega_q-\omega)^{-1}] +[N(\omega_q)+f(\omega)][(-\omega'+\omega_q+\omega)^{-1} -(-\omega'+\omega_q-\omega)^{-1}]\}, \quad (2a)$$

$$\Delta(\omega) = [Z(\omega)]^{-1} \int_0^\infty \frac{d\omega'}{\omega'} \times \mathrm{Re}[\Delta(\omega')] \int_0^{\omega_0} d\omega_q\, \alpha^2(\omega_q) F(\omega_q) \times\{[N(\omega_q)+f(-\omega')][(\omega'+\omega_q+\omega)^{-1}+(\omega'+\omega_q-\omega)^{-1}] -[N(\omega_q)+f(\omega')][(-\omega'+\omega_q+\omega)^{-1} +(-\omega'+\omega_q-\omega)^{-1}]\} - \frac{N(0)V_c}{Z(\omega)} \int_0^{E_B} \frac{d\omega'}{\omega'} \times \mathrm{Re}[\Delta(\omega')][1-2f(\omega')], \quad (2b)$$

where $F(\omega_q)$ is the phonon density of states, ω_0 is the maximum phonon frequency, $\alpha^2(\omega_q)$ is an average of the electron-phonon interaction, V_c is the matrix element of the screened Coulomb interaction averaged over the Fermi surface, E_B is the electronic bandwidth, and $N(\omega)$ and $f(\omega)$ are the Bose and Fermi occupation probabilities $[\exp(\omega/kT_c)\mp 1]^{-1}$. The screened Coulomb interaction is described by the parameters $N(0)V_c$ and E_B, and the electron-phonon interaction by the function $\alpha^2(\omega_q)F(\omega_q)$, which we will discuss in more detail below.

We find an approximate solution to Eq. (2) by substituting a trial function for $\Delta(\omega)$ on the right-hand side of (2) and computing $\Delta(\omega)$ by performing the indicated integrations. We then require that the trial $\Delta(\omega)$ and the computed $\Delta(\omega)$ be as consistent as possible. Such a procedure was followed by Morel and Anderson,[6] who, in fact, used a better trial function than we will take; we depend more on the accurate numerical results of the next section. We choose

$$\Delta_t(\omega) = \Delta_0, \quad 0<\omega<\omega_0 \qquad = \Delta_\infty, \quad \omega_0<\omega \quad (3)$$

and compute $\Delta(0)$ and $\Delta(\infty)$ from Eq. (2). Neglecting

[1] J. Bardeen, L. N. Cooper, and J. R. Schrieffer, Phys. Rev. **106**, 162 (1957); **108**, 1175 (1957).
[2] A. B. Migdal, Zh. Eksperim. i Teor. Fiz. **34**, 1438 (1958) [English transl.: Soviet Phys.—JETP **7**, 996 (1958)].
[3] G. M. Eliashberg, Zh. Eksperim. i Teor. Fiz. **38**, 966 (1960); **39**, 1437 (1960) [English transls.: Soviet Phys.—JETP **11**, 696 (1960); **12**, 1000 (1961)].
[4] Y. Nambu, Phys. Rev. **117**, 648 (1960).
[5] L. P. Gorkov, Zh. Eksperim. i Teor. Fiz. **34**, 735 (1958) [English transl.: Soviet Phys.—JETP **7**, 505 (1958)].
[6] P. Morel and P. W. Anderson, Phys. Rev. **125**, 1263 (1962).
[7] J. R. Schrieffer, *Theory of Superconductivity* (W. A. Benjamin, Inc., New York, 1964).
[8] J. R. Schrieffer, D. J. Scalapino, and J. W. Wilkins, Phys. Rev. Letters **10**, 336 (1963); D. J. Scalapino, J. R. Schrieffer, and J. W. Wilkins, Phys. Rev. **148**, 263 (1966).
[9] W. L. McMillan and J. M. Rowell, Phys. Rev. Letters **14**, 108 (1965); also (to be published).
[10] J. C. Swihart, D. J. Scalapino, and Y. Wada, Phys. Rev. Letters **14**, 106 (1965).
[11] V. Ambegaokar and L. Tewordt, Phys. Rev. **134**, A805 (1964).
[12] D. J. Scalapino, Y. Wada, and J. C. Swihart, Phys. Rev. Letters **14**, 102 (1965).

the thermal phonons, we have three contributions to $\Delta(0)$:

$$\Delta^1(0)=[Z(0)]^{-1}\int_0^{\omega_0}\frac{d\omega'}{\omega'}\,\Delta_0\int_0^{\omega_0}d\omega_q\,\alpha^2(\omega_q)F(\omega_q)$$
$$\times\{f(-\omega')(\omega'+\omega_q)^{-1}-f(\omega')(-\omega'+\omega_q)^{-1}\}$$
$$\cong\frac{\Delta_0}{Z(0)}\int_0^{\omega_0}\frac{d\omega'}{\omega'}\tanh\left(\frac{\omega'}{2T_c}\right).2\int_0^{\omega_0}\frac{d\omega_q\,\alpha^2(\omega_q)F(\omega_q)}{\omega_q}$$
$$\cong[\Delta_0\lambda/Z(0)]\ln(\omega_0/T_c). \tag{4}$$

The dominant contribution to the ω' integral is from small ω', and we neglect ω' relative to ω_q in the phonon propagators $(\omega'+\omega_q)^{-1}$. The natural definition of a dimensionless electron-phonon coupling constant is

$$\lambda\equiv 2\int_0^{\omega_0}\alpha^2(\omega_q)F(\omega_q)\,\frac{d\omega_q}{\omega_q}, \tag{5}$$

and λ corresponds roughly to the $N(0)V$ of the BCS model. Further, we have

$$\Delta^2(0)=[Z(0)]^{-1}\int_{\omega_0}^{\infty}\frac{d\omega'}{\omega'}\,\Delta_\infty\int_0^{\omega_0}d\omega_q\,\alpha^2(\omega_q)F(\omega_q)\,\frac{2}{\omega'+\omega_q}$$
$$\cong[\Delta_\infty/Z(0)](\langle\omega\rangle\lambda/\omega_0), \tag{6}$$

where $\langle\omega\rangle$ is an average phonon frequency;

$$\langle\omega\rangle=\int_0^{\omega_0}d\omega_q\,\alpha^2(\omega_q)F(\omega_q)\Big/\int_0^{\omega_0}\frac{d\omega_q}{\omega_q}\,\alpha^2(\omega_q)F(\omega_q)$$
$$\cong 0.5\omega_0, \tag{7}$$

and we have neglected ω_q relative to ω'. The first two contributions are from the electron-phonon interaction; the third term from the Coulomb interaction is

$$\Delta^3(0)=-[N(0)V_c/Z(0)]$$
$$\times[\Delta_0\ln(\omega_0/T_c)+\Delta_\infty\ln(E_B/\omega_0)]. \tag{8}$$

At high energies the only contribution is from the Coulomb interaction:

$$\Delta(\infty)=-[N(0)V_c/Z(\infty)]$$
$$\times[\Delta_0\ln(\omega_0/T_c)+\Delta_\infty\ln(E_B/\omega_0)]. \tag{9}$$

The renormalization is easily found to be

$$Z(0)=1+\lambda,\qquad Z(\infty)=1. \tag{10}$$

We satisfy our consistency requirement at low and high energies:

$$\Delta(0)=\Delta_0$$
$$=[\Delta_0\lambda/Z(0)]\ln(\omega_0/T_c)+[\Delta_\infty/Z(0)](\langle\omega\rangle/\omega_0)\lambda$$
$$-[N(0)V_c/Z(0)][\Delta_0\ln(\omega_0/T_c)+\Delta\ln(E_B/\omega_0)], \tag{11}$$

$$\Delta(\infty)=\Delta_\infty$$
$$=-N(0)V_c[\Delta_0\ln(\omega_0/T_c)+\Delta_\infty\ln(E_B/\omega_0)]$$
$$=-\frac{N(0)V_c\Delta_0\ln(\omega_0/T_c)}{1+N(0)V_c\ln(E_B/\omega_0)}$$
$$=-\mu^*\Delta_0\ln(\omega_0/T_c), \tag{12}$$

where μ^* is the Coulomb pseudopotential of Morel and Anderson[6]

$$\mu^*=\frac{N(0)V_c}{1+N(0)V_c\ln(E_B/\omega_0)}. \tag{13}$$

Substituting (12) into (11), we find

$$\Delta_0=\frac{\Delta_0[\lambda-\mu^*-\mu^*\lambda(\langle\omega\rangle/\omega_0)]\ln(\omega_0/T_c)}{1+\lambda}. \tag{14}$$

The strong-coupling formula analogous to Eq. (1) is then

$$\frac{T_c}{\omega_0}=\exp\left(\frac{-(1+\lambda)}{\lambda-\mu^*-(\langle\omega\rangle/\omega_0)\lambda\mu^*}\right). \tag{15}$$

In weak coupling ($\lambda\ll 1$), Eq. (15) reduces to the BCS result with $\lambda-\mu^*$ playing the role of $N(0)V$. The strong-coupling features are (1) that the interactions are renormalized by $Z=1+\lambda$ and (2) that the Coulomb interaction changes the gap function in such a way that the phonon contribution is reduced from λ to $\lambda[1-(\langle\omega\rangle/\omega_0)\mu^*]$.

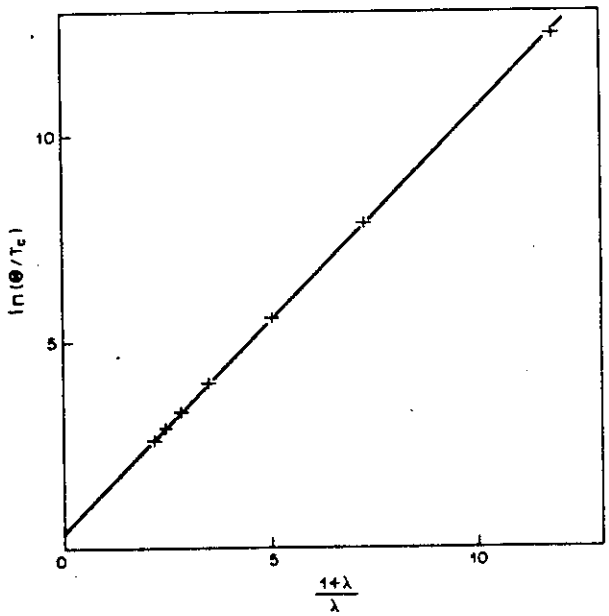

FIG. 1. The logarithm of Θ/T_c versus $(1+\lambda)/\lambda$ from a solution of the integral equations of the strong-coupled theory with $\mu^*=0$. The straight-line fit determines the constants (1.04 and 1.45) in the theoretical formula [(Eq. (18)].

III. NUMERICAL RESULTS

In order to find a more accurate solution of the gap equation, we go to the computer. We solve Eq. (2) by

TABLE I. Values of the coupling constant λ for various values of the Coulomb term μ^* and transition temperature T_c (in °K).

T_c \ μ^*	0	0.088	0.149	0.157	0.245
20	0.85	1.12	1.34		
15	0.68	0.93	1.12		1.47
10	0.55	0.75	0.91		1.20
5	0.40	0.58		0.72	
1	0.25	0.39		0.50	
0.1	0.16	0.28		0.38	
0.001	0.09			0.25	

a simple iterative procedure. We write (2) in the form

$$\Delta_{n+1}(\omega)=\int d\omega'\, K(\omega,\omega')\Delta_n(\omega'), \tag{16}$$

and choose $\Delta_1(\omega)$ to be the solution found in Sec. II. We substitute $\Delta_1(\omega)$ into the right-hand side of (16) and perform the indicated integration to find $\Delta_2(\omega)$, which is, we hope, closer to true solution. We find, in fact, that after four to eight iterations, $\Delta(\omega)$ has converged in the third decimal place. During the iteration it is convenient to fix T_c and μ^* and to adjust α^2 at each stage so that $\Delta_{n+1}(0)=\Delta_n(0)$. We must choose a particular $\alpha^2(\omega_q)F(\omega_q)$, and, since we will be interested in the bcc transition-metal alloys in the next section, we take $F(\omega_q)$ to be the phonon density of states of Nb found from the neutron work.[13] $\alpha^2(\omega_q)$ is taken to be a constant α^2 over most of the phonon spectrum; however, we take $\alpha^2F(\omega)=0$ for $\omega<100$°K to eliminate the coupling to the long-wavelength transverse phonons (see Fig. 4). We have performed the numerical calculations for several values of T_c and μ^* with T_c in the range 10^{-3} °K$<T_c<20$°K and μ^* between 0 and 0.2. The results for λ for various values of T_c and μ^* are given in Table I. Instead of plotting the numerical data as a family of curves, we will use the analytic formula (15) to fit the data. A plot (Fig. 1) of $\ln(\Theta/T_c)$ versus $(1+\lambda)/\lambda$ for $\mu^*=0$ yields a straight line with a slope of 1.04 and an intercept of $0.37=\ln 1.45$. In order to determine the constant $\langle\omega\rangle/\omega_0$ from the numerical data, we plot in Fig. 2 the quantity

$$y=\left(\lambda-\frac{1.04(1+\lambda)}{\ln(\Theta/1.45T_c)}\right)\Big/\mu^* \tag{17}$$

[which should be equal to $1+(\langle\omega\rangle/\omega_0)\lambda$] versus λ. A straight line with a slope of $\langle\omega\rangle/\omega_0=0.62$ and an intercept of 1 provides a good fit to the numerical data. The scatter of the points about the straight line is partly due to numerical inaccuracies of the computer program which are magnified in taking the difference to calculate y. The final formula for the transition temperature is then

$$T_c=\frac{\Theta}{1.45}\exp\left[-\frac{1.04(1+\lambda)}{\lambda-\mu^*(1+0.62\lambda)}\right]. \tag{18}$$

We have used the Debye Θ for the characteristic phonon frequency. We could just as well have used the maximum phonon frequency ω_0 or the average phonon frequency $\langle\omega\rangle$ [see Eq. (24) below]. For niobium, $\Theta=277$°K, $\omega_0=330$°K, and $\langle\omega\rangle=230$°K. We illustrate the accuracy of this analytic formula by plotting $y'=1.04(1+\lambda)/\ln(\Theta/1.45T_c)$ versus λ in Fig. 3. The analytic formula gives the family of straight lines $y'=-\mu^*+(1-0.62\mu^*)\lambda$ for a fixed μ^*. The numerical data points (for the same μ^* values) are shown by crosses. The analytic formula does give a good fit to the numerical values over a wide range of parameters.

The energy-gap function $\Delta(\omega)$ for a typical set of parameters ($\lambda=0.91$, $\mu^*=0.149$, $T_c=10$°K) corresponding roughly to those of Nb is shown in Fig. 4, together with the phonon density of states of Nb.

Since we will find empirical values of λ in the next section, we are interested in the definition of λ in terms of the electronic matrix elements and the phonon frequencies. We have used $\alpha^2(\omega)F(\omega)$, which is defined by

$$\alpha^2(\omega)F(\omega)=\int_S\frac{d^2p}{v_F}\int_{S'}\frac{d^2p'}{(2\pi\hbar)^3v_{F'}}\sum_\nu g_{pp'\nu}{}^2\delta(\omega-\omega_{p-p'\nu})\Big/\int_S\frac{d^2p}{v_F}, \tag{19}$$

where the integral $\int d^2p$ is taken over the Fermi surface and the electron-phonon matrix elements are given by[14]

$$g_{pp'\nu}=(\hbar/2MNV\omega_{p-p'\nu})^{1/2}\mathcal{g}_\nu(p,p'), \tag{20}$$

where $\mathcal{g}_\nu(pp')$ is the electronic matrix element of the change in the crystal potential $\mathcal{U}$ as one atom is moved:

$$\mathcal{g}_\nu(pp')=\int\psi_p{}^*(\boldsymbol{\varepsilon}_{p-p'\nu}\cdot\nabla\mathcal{U})\psi_{p'}d\mathbf{r}. \tag{21}$$

Note that g^2 is inversely proportional to the phonon energy $\omega_{p-p'}$, so that the first moment of $\alpha^2(\omega)F(\omega)$ is independent of the phonon frequencies:

$$\int_0^\infty d\omega\,\omega\alpha^2(\omega)F(\omega)=\int\frac{d^2p}{v_F}\int\frac{d^2p'}{(2\pi)^3v_{F'}}\sum_\nu\frac{\hbar}{2MNV}\mathcal{g}_\nu{}^2(pp')\Big/\int\frac{d^2p}{v_F}$$

$$=\frac{N(0)\hbar\langle\mathcal{g}^2\rangle}{2M}. \tag{22}$$

[13] Y. Nakagawa and A. D. B. Woods, Phys. Rev. Letters 11, 271 (1963).
[14] J. M. Ziman, *Electrons and Phonons* (Oxford University Press, London, 1960), p. 182.

Here $\langle \mathcal{I}^2 \rangle$ is the average over the Fermi surface of the square of the electronic matrix element (21). Finally, from the definition of λ, we have

$$\lambda = 2\int \frac{d\omega\, \alpha^2(\omega) F(\omega)}{\omega} = \frac{N(0)\langle \mathcal{I}^2 \rangle}{M\langle \omega^2 \rangle}, \qquad (23)$$

where $\langle \omega^2 \rangle$ is an average of the square of the phonon frequency:

$$\langle \omega^2 \rangle = \int d\omega\, \omega\alpha^2(\omega) F(\omega) \Big/ \int \frac{d\omega\, \alpha^2(\omega) F(\omega)}{\omega}$$

$$\cong \int d\omega\, \omega F(\omega) \Big/ \int \frac{d\omega\, F(\omega)}{\omega}. \qquad (24)$$

The transition temperature (18) depends on the isotopic mass[6,15] directly through the factor Θ and implicitly through the ω_0 dependence of μ^*. Using (18) and (13), we find $T_c \propto M^{-\alpha}$, with

$$\alpha = \frac{1}{2}\left(1 - \frac{(1+\lambda)(1+0.62\lambda)\mu^{*2}}{[\lambda - \mu^*(1+0.62\lambda)]^2}\right)$$

$$= \frac{1}{2}\left[1 - \left(\mu^* \ln \frac{\Theta}{1.45 T_c}\right)^2 \frac{1+0.62\lambda}{1+\lambda}\right], \qquad (25)$$

which differs very little from the weak-coupling result.

The velocity of electrons near the Fermi surface is renormalized by the electron-phonon interaction. To see this, we find the self-energy for electrons in the normal state [Eq. (2a)] for $T=0$ and $\omega \ll \omega_0$:

$$\xi(\omega) \cong -\lambda\omega. \qquad (26)$$

The energy of the electronic excitations is determined from the poles of the Green's function, or from

$$\omega - \epsilon_k - \xi(\omega) = 0, \qquad (27)$$

where ϵ_k is the energy of the Bloch state (measured from the Fermi energy) with momentum k. Substituting (26) into (27), we find for the energy ω of the elementary excitation,

$$\omega = \epsilon_k/(1+\lambda). \qquad (28)$$

The electronic heat-capacity coefficient γ,[2,16] the cyclotron masses,[17,18], and the Fermi velocity measured in the Tomash-Rowell experiments[19–22] are all renormalized by the factor $(1+\lambda)$.

This completes the theoretical portion of the paper, and we will summarize the results. Our central result is Eq. (18), which expresses T_c in terms of a characteristic phonon energy Θ, the electron-phonon coupling constant λ, and the Coulomb "pseudopotential" μ^*. This formula was derived from accurate numerical solutions of the integral equations of the (accurate) theory of superconductivity with, however, a special assumption about the shape of the phonon density of states. The superconductor was assumed to be isotropic, but this is not a serious approximation. The definitions of λ and μ^* in terms of the basic metallic properties are given in Eqs. (23) and (13). Several observable properties of the metal are modified from their "band-structure" values by the electron-phonon interaction. The velocity of electrons near the Fermi surface is reduced by the factor $(1+\lambda)$; this velocity is measured in the Tomash-effect experiments. The electronic heat capacity and cyclotron mass are enhanced by the factor $(1+\lambda)$. The cyclotron-mass enhancement is in fact anisotropic

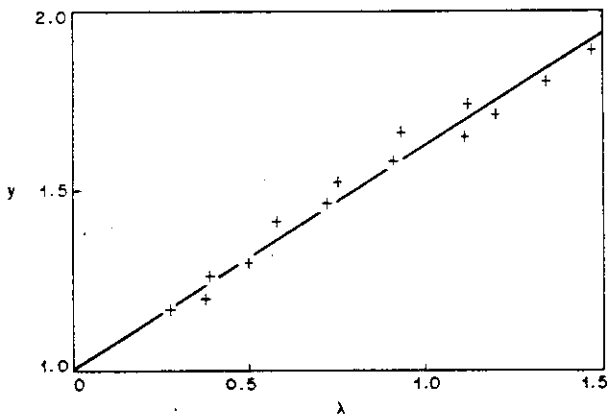

FIG. 2. The quantity y defined in Eq. (17) versus λ; the straight-line fit determines the third parameter (0.62) in the theoretical formula [Eq. (18)].

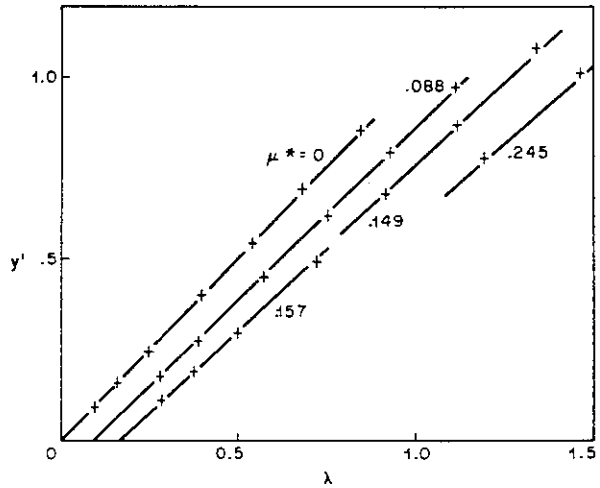

FIG. 3. The quantity $y' = 1.04(1+\lambda)/\ln(\Theta/1.45T_c)$ versus λ according to (+++), the computer program, and (——), the analytic formula [Eq. (18)], demonstrating that the analytic formula does fit the numerical results.

[15] J. W. Garland, Jr., Phys. Rev. Letters **11**, 114 (1963).

[16] G. M. Eliashberg, Zh. Eksperim. i Teor. Fiz. **43**, 1005 (1962) [English transl.: Soviet Phys.—JETP **16**, 780 (1963)].

[17] S. Nakajima and M. Watabe, Progr. Theoret. Phys. (Kyoto) **30**, 271 (1963).

[18] R. E. Prange and L. P. Kadanoff, Phys. Rev. **134**, A566 (1964).

[19] W. J. Tomasch, Phys. Rev. Letters **15**, 672 (1965); **16**, 16 (1966).

[20] W. L. McMillan and P. W. Anderson, Phys. Rev. Letters **6**, 85 (1966).

[21] W. J. Tomasch and T. Wolfram, Phys. Rev. Letters **16**, 352 (1966).

[22] J. M. Rowell and W. L. McMillan, Phys. Rev. Letters **16**, 453 (1966).

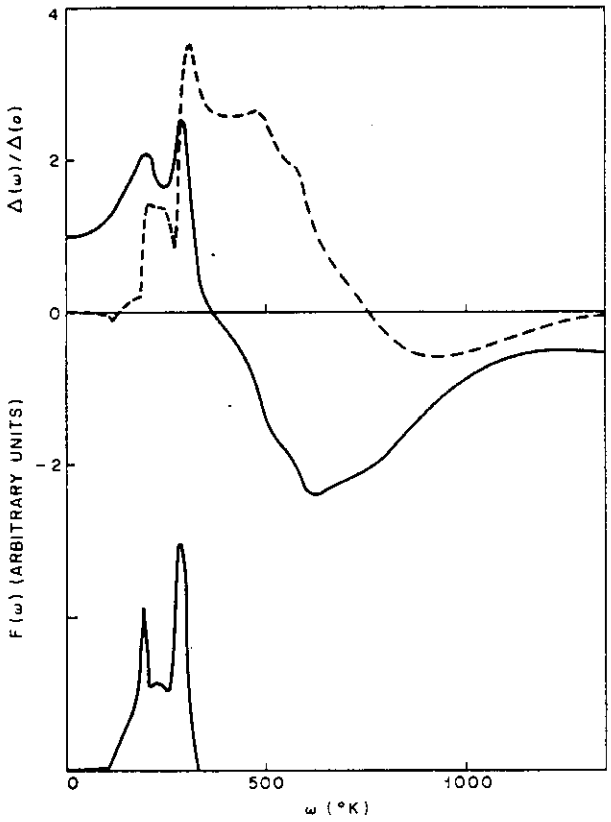

FIG. 4. The real (——) and imaginary (– – –) parts of the energy-gap function versus energy at the transition temperature for parameters (T_c=10°K, λ=0.91, μ^*=0.149) corresponding roughly to niobium, together with the phonon density of states for niobium used in the calculations.

and will vary from orbit to orbit; λ is an isotropically averaged quantity, and $(1+\lambda)$ gives an average enhancement factor. The strong-coupled formula (25) for the isotope shift was obtained directly from (18) and (13), and is numerically very close to the weak-coupling result.

IV. EMPIRICAL RESULTS

We begin now the empirical portion of the paper, making use of the theoretical equations and experimental results to extract the coupling constants λ and μ^*. We first determine μ^* for those few metals for which the isotope shift has been measured. Then, taking reasonable values of μ^* for the other metals, we will find empirical values of λ from T_c and Θ. Finally, we use these empirical numbers for λ to estimate the "phonon enhancement" of the electronic heat capacity γ and deduce from the measured γ the bare or "band-structure" electronic density of states at the Fermi energy.

Neglecting the "strong-coupling" correction $(1+0.62\lambda)/(1+\lambda)$ in Eq. (25), we find an expression for the Coulomb pseudopotential μ^* in terms of the isotope-shift coefficient α, the transition temperature, and the Debye Θ:

$$\mu^*=(1-2\alpha)^{1/2}/\ln(\Theta/1.45T_c). \qquad (29)$$

The experimental values of α, T_c, and Θ are given in Table II, together with the empirical value of μ^* obtained using Eq. (29). For the transition metals, we see that there is some variation about the average value of $\mu^*=0.13$. The higher T_c transition metals have higher densities of states and smaller effective bandwidths, and somewhat larger values of μ^* are appropriate. However, for these metals, μ^* is less important relative to λ, and we take below the value 0.13 for all transition metals. For the nearly-free-electron metals, the theoretical estimate $\mu^*=0.1$ is reasonable, and this is confirmed by the empirical μ^* for zinc.

Next, we rewrite Eq. (18) in a convenient form for finding an empirical electron-phonon coupling constant λ from the experimentally determined transition temperature T_c and Debye Θ:

$$\lambda=\frac{1.04+\mu^*\ln(\Theta/1.45T_c)}{(1-0.62\mu^*)\ln(\Theta/1.45T_c)-1.04}. \qquad (30)$$

Here we use $\mu^*=0.13(0.1)$ for the transition (polyvalent) metals. The experimental T_c and Θ are listed in Table III for the superconducting metals, together with the empirical coupling constant λ found using Eq. (30). The coupling constant found in this way is reliable for weak and intermediate coupling strengths $\lambda<1$. However, for the strong-coupled case $\lambda>1$, the resulting λ is sensitive to the details of the phonon spectrum, and it is desirable to have more information about the phonon density of states than just the Debye Θ. For lead, where the phonon density of states is known from the analysis of the tunneling experiments to be quite similar to that for niobium, Eq. (30) works reasonably well; the coupling constant deduced from the tunneling data is 1.3, and Eq. (30) yields 1.1. For mercury, however, the tunneling experiment yields a phonon spectrum quite different from niobium, and Eq. (30) fails; the tunneling experiment gives $\lambda=1.6$, whereas Eq. (30)

TABLE II. Empirical values of the Coulomb pseudopotential μ^* found from the isotope shift α, T_c, and Θ using Eq. (29).

Metal	α	T_c (°K)	Θ (°K)	μ^*	Reference
Zr	0.00±0.05	0.55	290	0.17	a
Mo	0.37±0.04	0.92	460	0.09	b
Re	0.38	1.69	415	0.10	c
Ru	0.0±0.15	0.49	550	0.15	d, e
Os	0.21	0.65	500	0.12	e
Zn	0.30±0.01	0.85	309	0.12	f

[a] E. Bucher, J. Muller, J. L. Olsen, and C. Palmy, Phys. Letters 15, 303 (1965).
[b] B. T. Matthias, T. H. Geballe, E. Corenzwit, and G. W. Hull, Jr., Phys. Rev. 129, 1025 (1963); E. Bucher and C. Palmy, Phys. Letters 24A, 340 (1967).
[c] E. Maxwell, Rev. Mod. Phys. 36, 144 (1964).
[d] T. H. Geballe, B. T. Matthias, G. W. Hull, Jr., and E. Corenzwit, Phys. Rev. Letters 6, 275 (1961); D. K. Finnemore and D. E. Mapother, *ibid.* 9, 288 (1962); J. W. Gibson and R. A. Hein, Phys. Rev. 141, 407 (1966).
[e] T. H. Geballe and B. T. Matthias, IBM J. Res. Develop. 6, 256 (1962); R. A. Hein and J. W. Gibson, Phys. Rev. 131, 1105 (1963).
[f] R. E. Fassnacht and J. R. Dillinger, Phys. Rev. Letters 17, 255 (1966).

TABLE III. Empirical values of the electron-phonon coupling constant λ and the "band-structure" density of states $N_{bs}(0)$ found from T_c, Θ, and γ for the superconducting metals.

Element	T_c (°K)	Θ (°K)	γ (mJ/mole °K²)	λ	$N_{bs}(0)$ (states/eV atom)	$N_{bs}(0)/N_{fe}(0)$	Reference
Be	0.026	1390	0.184	0.23	0.032	0.31	a, b
Al	1.16	428	1.35	0.38	0.208	1.08	c
Zn	0.85	309	0.64	0.38	0.098	0.61	d
Ga	1.08	325	0.60	0.40	0.091	0.46	e
Cd	0.52	209	0.69	0.38	0.106	0.53	e
In	3.40	112	1.69	0.69	0.212	0.89	f
Sn	3.72	200	1.80	0.60	0.238	0.82	g
Hg	4.16	72	1.79	1.00	0.146*	0.70	h
Tl	2.38	79	1.47	0.71	0.182	0.66	h
Pb	7.19	105	3.00	1.12	0.276*	0.87	i
Ti	0.39	425	3.32	0.38	0.51		j, k
V	5.30	399	9.9	0.60	1.31		j, k
Zr	0.55	290	2.78	0.41	0.42		j, k
Nb	9.22	277	7.8	0.82	0.91		k
Mo	0.92	460	1.83	0.41	0.28		j, k
Ru	0.49	550	3.0	0.38	0.46		j, k
Hf	0.09	252	2.16	0.34	0.34		l, k
Ta	4.48	258	6.0	0.65	0.77		j, k
W	0.012	390	0.90	0.28	0.15		m, k
Re	1.69	415	2.3	0.46	0.33		j, k
Os	0.65	500	2.3	0.39	0.35		j, k
Ir	0.14	420	3.2	0.34	0.51		j, k

[a] R. L. Falge, Jr., Phys. Letters **24**, 579 (1967).
[b] E. Gmelin, Compt. Rend. **259**, 3459 (1964).
[c] Norman E. Phillips, Phys. Rev. **114**, 676 (1959).
[d] G. Seidel and P. H. Keesom, Phys. Rev. **112**, 1083 (1958).
[e] Norman E. Phillips, Phys. Rev. **134**, A385 (1964).
[f] H. R. O'Neal and N. E. Phillips, Phys. Rev. **137**, A748 (1965).
[g] C. A. Bryant and P. H. Keesom, Phys. Rev. **123**, 491 (1961).
[h] B. J. C. van der Hoeven, Jr., and P. H. Keesom, Phys. Rev. **135**, A631 (1964).
[i] B. J. C. van der Hoeven, Jr., and P. H. Keesom, Phys. Rev. **137**, A103 (1965).
[j] B. W. Roberts, *Progress in Cryogenics* (Heywood and Co., Ltd., London, 1964).
[k] F. Heininger, E. Bucher, and J. Muller, Physik Kondensierten Materie **5**, 243 (1966).
[l] K. Andres (private communication).
[m] R. T. Johnson, O. E. Vilches, J. C. Wheatley, and S. Gygax, Phys. Rev. Letters **16**, 101 (1966).

gives $\lambda = 1.0$. The point is that whenever Eq. (30) yields a coupling constant greater than 1 and there is no information available for the phonon density of states, the results should be treated with some caution.

The electronic heat-capacity coefficient γ is proportional to the electronic density of states at the Fermi surface (the "band-structure" density of states) times the enhancement factor $(1+\lambda)$ from the electron-phonon interaction. If λ and γ are known, we can find the band-structure density of states $N_{bs}(0)$:

$$N_{bs}(0) = 3\gamma/2\pi^2 k_B^2(1+\lambda). \tag{31}$$

Strictly speaking, $N_{bs}(0)$ contains the enhancement due to the Coulomb interactions between electrons. In Table III are listed the experimental heat capacity γ and the empirical electronic density deduced from Eq. (31) and the empirical coupling constant λ.[23] For lead and mercury, we have used the λ found from the tunneling experiments. For the polyvalent metals, we list the ratio of $N_{bs}(0)$ to the electronic density of states at the Fermi surface from the free-electron model

$$N_{fe}(0) = \tfrac{3}{4}(Z/E_F), \tag{32}$$

where Z is the valence and E_F the Fermi energy.

[23] J. W. Garland, Jr., has performed a similar service (to be published).

This procedure for extracting the band-structure density of states is particularly interesting when the experimental data (T_c, Θ, γ) are available for a series of alloys with the same crystal structure. Consider the bcc alloy system Ta–W. According to the rigid-band model, which seems quite reasonable for the alloy systems considered here, the band structures of Ta and W are very similar, and in alloying from Ta to W, one is merely increasing the Fermi energy so that the volume contained in the Fermi surface increases from 5 electrons/atom to 6 electrons/atom. Using the same procedure described in the above paragraphs for metals, we can find the band-structure density of states at the Fermi energy for each alloy and plot out the band-structure density of states as a function of either electron/atom ratio or energy. It is quite reasonable to compare this empirical density of states versus energy curve with that calculated from the computed band structure of either Ta or W. There are sufficient data available to construct the density of states versus electron/atom ratio for four alloy series of the transition metals.

(1) $N_{bs}(0)$ for the bcc $3d$ transition-metal alloys of Ti–V and V–Cr are given in Table IV and plotted in Fig. 5. The V–Cr alloys with more than 60% Cr are not superconducting above 0.025°K, and the coupling con-

TABLE IV. Empirical values of λ and $N_{bs}(0)$ found from T_c, Θ, and γ for the bcc 3*d* transition-metal alloys and for "paramagnetic" chromium. The values of λ in parentheses were obtained by extrapolation.

Alloy	% second metal	T_c (°K)	Θ (°K)	γ (mJ/mole °K²)	λ	$N_{bs}(0)$ (states/ eV atom)	Reference
TiV	20	3.5		6.9	0.54	0.95	a
	30	6.14		10.0	0.62	1.31	a
	50	7.30		10.8	0.65	1.39	a
	75	7.16		10.6	0.65	1.36	a
	85	7.02		10.3	0.65	1.32	a
VCr	10	3.21	370	8.15	0.53	1.13	b
	20	1.90	400	7.15	0.48	1.02	b
	25	1.36	425	6.75	0.45	0.99	b
	40	0.37	450	5.4	0.38	0.83	b
	50	0.10	470	4.85	0.33	0.77	b
	60	<0.025		4.0	(0.28)	0.67	b
	80			2.1	(0.20)	0.37	c
	90			2.07	(0.20)	0.37	c
	94.5			2.33	(0.20)	0.41	c
"Cr"				2.9	(0.25)	0.49	c

[a] C. H. Cheng, K. P. Gupta, E. C. van Reuth, and P. A. Beck, Phys. Rev. 127, 2030 (1962).
[b] K. Andres and E. Bucher (private communication).
[c] F. Heiniger, Physik Kondensierten Materie 5, 285 (1966).

stants are found by extrapolation. The γ value for Cr is that for "paramagnetic" Cr found by extrapolating the γ for paramagnetic Mo–Cr alloys.

(2) The most complete data are for the bcc 4*d* transition-metal alloys of Zr–Nb, Nb–Mo, and Mo–Tc (Table V and Fig. 6). We have used, in addition, the 4*d*–5*d* alloys of Mo–Re which should give $N_{bs}(0)$ values reasonably close to Mo–Tc. Heiniger *et al.*[24] have noted that the γ values for Zr–Rh alloys appear to lie on the same curve as for the Zr–Nb alloys, and we have in-

TABLE V. Empirical values of λ and $N_{bs}(0)$ found from T_c, Θ, and γ for the bcc 4*d* transition-metal alloys.

Alloy	% second metal	T_c (°K)	Θ (°K)	γ (mJ/mole °K²)	λ	$N_{bs}(0)$ (states/ eV atom)	Reference
ZrNb	50	9.3	238	8.3	0.88	0.93	a
	75	10.8	246	8.9	0.93	0.98	a
NbMo	15	5.85	265	6.3	0.70	0.79	b
	40	0.60	371	2.87	0.41	0.43	b
	60	0.05	429	1.62	0.31	0.26	b
	70	0.016	442	1.46	0.29	0.24	b
	80	0.095	461	1.49	0.33	0.24	b
	90	0.30	487	1.67	0.36	0.26	b
MoRe	5	1.5	450	2.2	0.45	0.32	c
	10	2.9	440	2.6	0.51	0.36	c
	20	8.5	420	3.8	0.68	0.48	c
	30	10.8	395	4.1	0.76	0.49	c
	40	12.6	340	4.4	0.86	0.50	c
	50	11.5	320	4.4	0.85	0.50	c
MoTc	50	12.6	300	4.6	0.91	0.51	c
ZrRh	3	3.1	244	3.62	0.59	0.48	d
	4	3.8	226	3.83	0.64	0.50	d
	5	4.8	210	5.08	0.70	0.63	d
	6	5.75	196	6.80	0.78	0.81	d
	7	5.95	192	7.36	0.80	0.87	d

[a] F. Heiniger, E. Bucher, and J. Muller, Physik Kondensierten Materie 5, 243 (1966); R. D. Blangher, J. K. Hulm, J. A. Rayne, B. W. Veal, and R. A. Hein, in *Proceedings of the Eighth International Conference on Low-Temperature Physics, London, 1962*, edited by R. O. Davies (Butterworths Scientific Publications, Ltd., London, 1963).
[b] B. W. Veal and J. K. Hulm, Ann. Acad. Sci. Fennicae A210, 108 (1966).
[c] F. J. Morin and J. P. Maita, Phys. Rev. 129, 1115 (1963).
[d] G. Dummer, Z. Physik 186, 249 (1965).

[24] F. Heiniger, E. Bucher, and J. Muller, Physik Kondensierten Materie 5, 243 (1966).

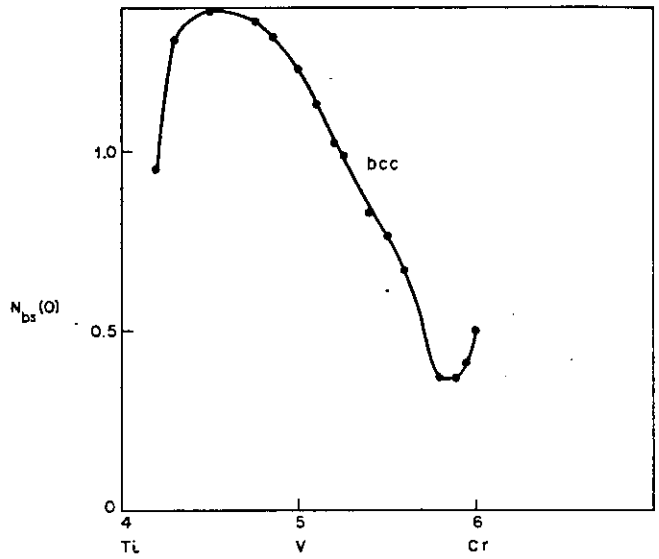

FIG. 5. The band-structure density of states versus electron/atom ratio for the bcc 3*d* transition-metal alloys from the data in Tables III and IV.

cluded those data as well, although it is by no means clear that the rigid-band model is valid for alloys of metals whose valence differs by 5.

(3) The values of $N_{bs}(0)$ for the bcc 5*d* alloys of Hf–Ta, Ta–W, and W–Re, as well as the hcp 5*d* alloys of W–Re and Re–Os, are given in Table VI and plotted in Fig. 7. Again it is necessary to interpolate for λ where the T_c has not been measured. The densities of states of the three bcc alloy series are similar, exhibiting a peak for electron/atom ratio $n=4.5$, a deep minimum near $n=5.8$, and a shoulder at $n=6.2$. Figure 8 shows a plot of the electron-phonon coupling constant λ versus electron/atom ratio, and Fig. 9 gives λ plotted versus density of states for these alloy series.

It is most interesting at this point to compare our empirical results with the theoretical density of states

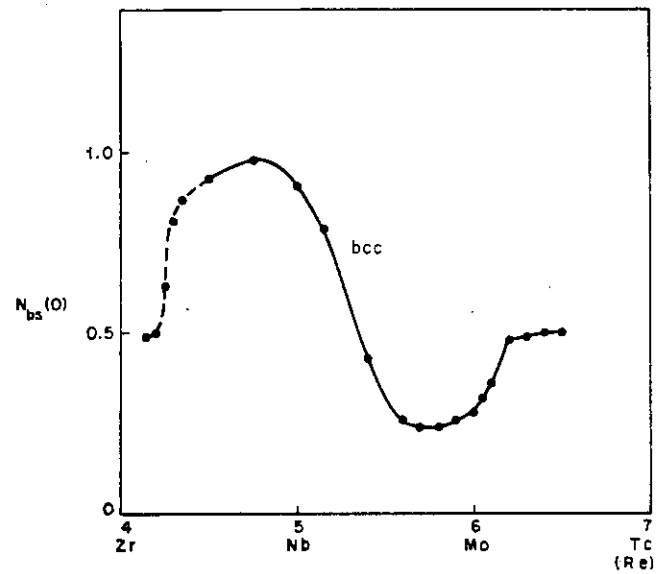

FIG. 6. The band-structure density of states versus electron/atom ratio for the bcc 4*d* transition-metal alloys from the data in Tables III and V.

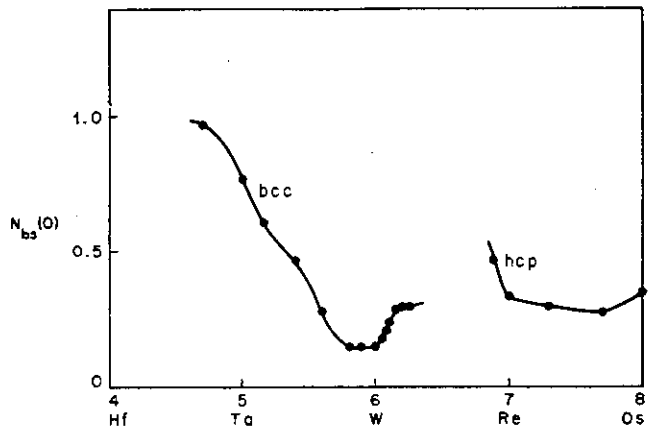

FIG. 7. The band-structure density of states versus electron/atom ratio for the bcc and hcp 5*d* transition-metal alloys from the data in Tables III and VI.

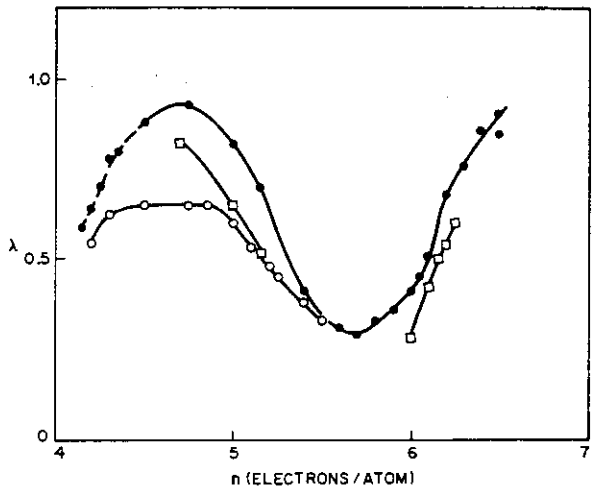

FIG. 8. The empirical electron-phonon coupling constant versus electron/atom ratio for the bcc 3*d* (○○○), 4*d* (●●●), and 5*d* (□□□) transition-metal alloys from the data in Tables III–VI.

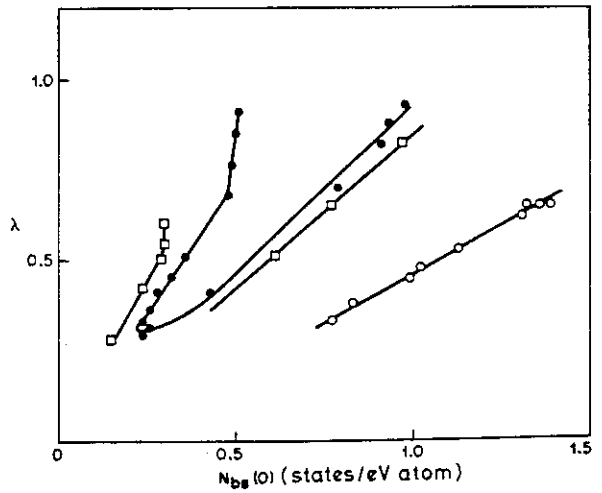

FIG. 9. The empirical electron-phonon coupling constant versus the band-structure density of states for the bcc 3*d* (○○○), 4*d* (●●●), and 5*d* (□□□) transition-metal alloys from the data in Tables III–IV.

TABLE VI. Empirical values of λ and $N_{bs}(0)$ found from T_c, Θ, and γ for the bcc (*hcp) 5*d* transition-metal alloys. The values of λ in parentheses were obtained by interpolation.

Alloy	% second metal	T_c (°K)	Θ (°K)	γ (mJ/mole °K²)	λ	$N_{bs}(0)$ (states/eV atom)	Reference
Hf–Ta	70	6.81	209	8.30	0.82	0.97	a, b
Ta–W	16	1.85	265	4.36	0.51	0.61	a, b
	40		291	3.08	(0.39)	0.47	a
	60		317	1.63	(0.25)	0.28	a
	80		354	0.88	(0.26)	0.15	a
	90		368	0.92	(0.27)	0.15	a
W–Re	5		380	1.14	(0.32)	0.18	a
	7.5		378	1.40	(0.38)	0.21	a
	10	0.7	375	1.63	0.42	0.24	a, b
	15	2.26	365	2.10	0.50	0.29	a, b
	20	3.20	359	2.20	0.54	0.30	a, b
	25	4.64	351	2.30	0.60	0.30	a, b
W–Re*	88	7.47	332	3.76	0.70	0.47	a, b
Re–Os*	30	1.45	351	2.05	0.47	0.30	a, b
Re–Os*	70		382	1.86	(0.42)	0.28	a

[a] E. F. Bucher, F. Heiniger, and J. Muller, in *Proceedings of the Ninth International Conference on Low-Temperature Physics, Columbus, Ohio,* edited by J. A. Daunt *et al.* (Plenum Press, Inc., New York, 1965), p. 1059.
[b] E. Bucher (private communication).

from band-structure calculations. Matthies[25] has calculated the band structure of tungsten using the augmented plane-wave (APW) method for two potentials (labeled W_1 and W_2), and has computed the electronic density of states versus energy. Figure 10 shows the theoretical density of states for potential W_2, together with the empirical density of states (solid circles) for the Hf–Ta–W–Re alloys from Tables III and VI. For the empirical data, the energy was determined from the electron/atom ratio, using the theoretical curve (dotted line of Fig. 10). As can be seen in Fig. 10, the agreement between the theoretical and empirical densities of states is excellent for this potential (W_2). The *d* band is about 25% narrower for potential W_1 than for W_2, and the density of states correspondingly higher. The shoulder at $n=6.15$ (Fig. 7) or at $E=1.17$ Ry (Fig. 10) is a critical point and can probably be identified with the saddle point in the Matthies band structure about half-way between the symmetry points H and N and lying just above the tungsten Fermi energy.

Matthies[26] has also computed the band structure and electronic density of states for hcp rhenium using the relativistic APW method. The theoretical density of states is in good agreement with the empirical data for the hcp W-Re-Os alloys (see Fig. 5 of Ref. 26).

V. ELECTRON-PHONON COUPLING CONSTANT

Having found empirical values of the electron-phonon coupling constant λ for a number of metals and alloys, we now wish to investigate the dependence of the coupling constant on the various metallic properties.

[25] L. F. Matthies, Phys. Rev. 139, A1893 (1965).
[26] L. F. Matthies, Phys. Rev. 151, 450 (1966).

A. Empirical Results

According to Eq. (23), in order to calculate the coupling constant, we need to know the electronic density of states $N_{bs}(0)$, an average phonon frequency $\langle\omega\rangle$, and an average squared electronic matrix element, $\langle\mathcal{I}^2\rangle$. The least accessible of these quantities is the last, $\langle\mathcal{I}^2\rangle$, and we will first adopt the empirical approach and determine $\langle\mathcal{I}^2\rangle$ from the experimental data for λ, $N(0)$, and $\langle\omega\rangle$. For this purpose the Debye Θ does not provide a sufficiently reliable estimate of the average phonon frequency, and we must restrict this discussion to those metals for which neutron scattering or electron tunneling measurements of the phonon frequencies are available. The phonon density of states of Nb (Fig. 4) is typical for fcc and bcc lattices, and for that case the average phonon frequency [Eq. (24)] is approximately the mean of the frequencies of the longitudinal and transverse peaks. In Table VII we give the average phonon frequency found in this way, together with the empirical λ and $N(0)$ values from Table III for the bcc transition metals, three polyvalent metals, and V_3Si. From these three empirical quantities, we find the empirical values for $\langle\mathcal{I}^2\rangle$ given in Table VII by rewriting Eq. (23)

$$\langle\mathcal{I}^2\rangle=[\lambda M\langle\omega^2\rangle/N(0)]. \tag{33}$$

Dimensionally, $\mathcal{I}$ is an electronic quantity with units of energy/length. The characteristic energy—the electronic-bandwidth or Fermi energy—is of the order of a few electron volts, and the characteristic length is the lattice spacing, a few angstroms; we expect $\mathcal{I}$ to be a few eV/Å, as observed. Note that for the bcc transition metals, $N(0)\langle\mathcal{I}^2\rangle$ (Table VII) is constant $\sim$7 eV/Å^2 within experimental uncertainty, even though $N(0)$ and

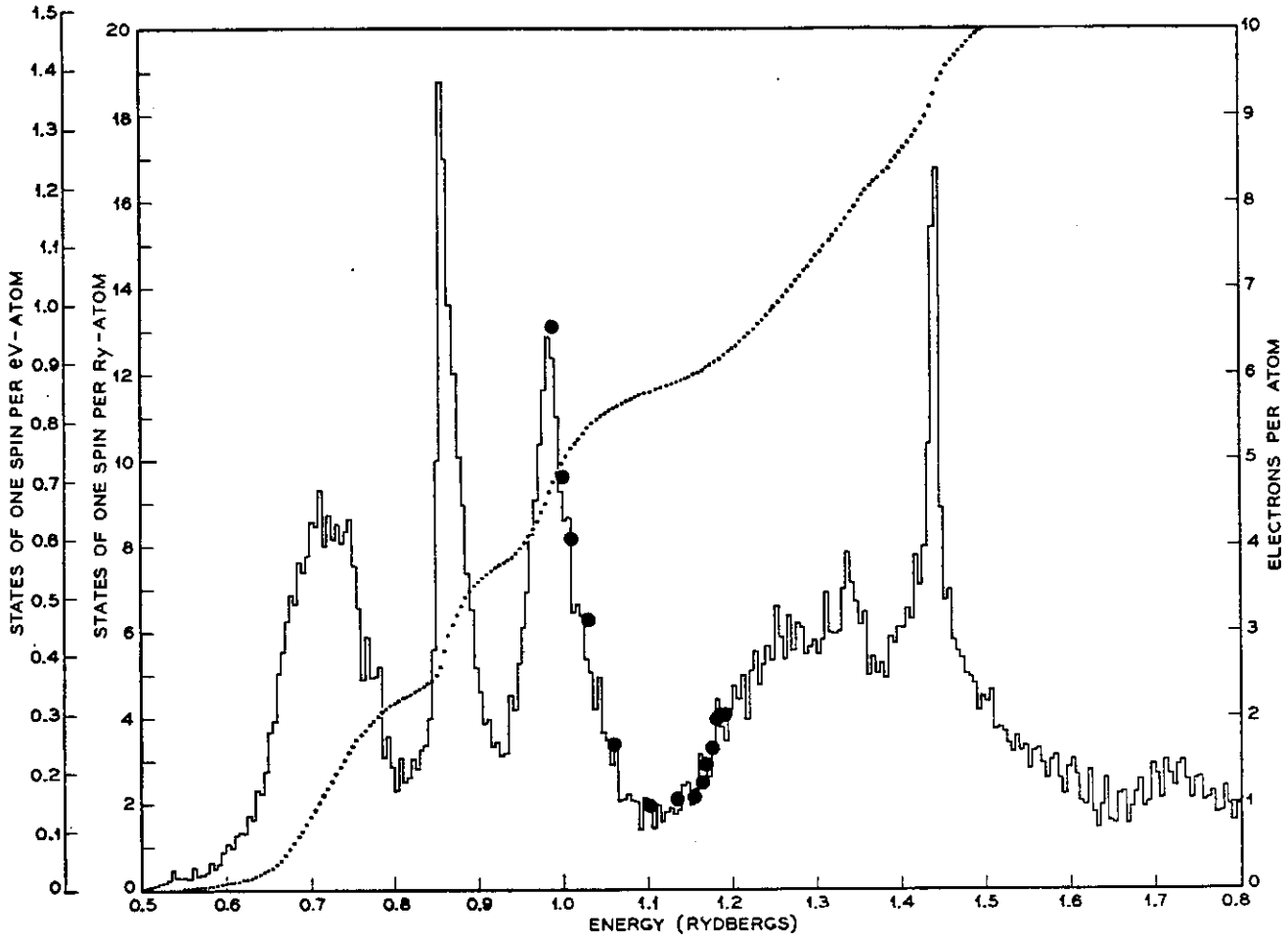

FIG. 10. The theoretical band-structure density of states versus energy for tungsten according to Matthies (Ref. 25), together with the empirical (solid-circles) data for the bcc 5*d* alloys from Tables III and VI.

$\langle \mathcal{I}^2 \rangle$ individually vary by a factor of 10 [for vanadium $N(0)\langle \mathcal{I}^2 \rangle$ is somewhat low, but the uncertainty in $\langle \mathcal{I}^2 \rangle$ because of the uncertainty in $\langle \omega \rangle$ is greater]. This is a remarkable result: We find empirically that for this class of materials, the electronic factor $N(0)\langle \mathcal{I}^2 \rangle$ remains constant and that the coupling constant (or transition temperature) is governed by the phonon factor $M\langle \omega^2 \rangle$ or by the stiffness of the lattice. This is in marked contrast to the statement that is usually made—that the coupling constant (or transition temperature) is

TABLE VII. Empirical values of the average electronic matrix element $\langle \mathcal{I}^2 \rangle$ found from λ, $N_{bs}(0)$, and $\langle \omega^2 \rangle^{1/2}$ using Eq. (33). The T_c, Θ, and γ values are taken from Table III.

Metal	T_c (°K)	T_c (°K)	γ (mJ/mole °K²)	λ	$N_{bs}(0)$ (states/eV atom)	$\langle \omega^2 \rangle^{1/2}$ (°K)	$\langle \mathcal{I}^2 \rangle$ (eV² Å^{-2})	$N(0)\langle \mathcal{I}^2 \rangle$ (eV Å^{-2})	Reference
V	5.30	399	9.9	0.60	1.31	290	3.5	4.6	a
Nb	9.22	277	7.8	0.82	0.91	230	7.9	7.2	b
Ta	4.48	258	6.0	0.65	0.77	170	7.9	6.1	c
Mo	0.92	460	1.83	0.41	0.275	310	24.6	6.8	d
W	0.012	390	0.90	0.29	0.148	250	42.5	6.3	e
Al	1.16	428	1.35	0.38	0.206	330	9.7	2.0	f
In	3.40	112	1.69	0.71	0.21	110	8.4	1.76	g
Pb	7.19	105	3.00	1.12	0.300	75	7.8	2.34	h, i
V_3Si	17	520	21[j]	0.82	2.33[j]	390	4.9	11.3	k, l

[a] K. C. Tuberfield and P. A. Engelstaff, Phys. Rev. **127**, 1017 (1962).
[b] Y. Nakagawa and A. D. B. Woods, Phys. Rev. Letters **11**, 271 (1963).
[c] A. D. B. Woods, Phys. Rev. **136**, A781 (1964).
[d] A. D. B. Woods, and S. H. Shen, Solid State Commun. **2**, 223 (1964).
[e] S. H. Shen and B. N. Brockhouse, Solid State Commun. **2**, 73 (1964).
[f] R. Stedman and G. Nilsson, Phys. Rev. **145**, 492 (1966).
[g] J. M. Rowell and W. L. McMillan (to be published).
[h] B. N. Brockhouse, T. Arase, G. Caglioti, K. R. Rao, and A. D. B. Woods, Phys. Rev. **128**, 1099 (1962).
[i] W. L. McMillan and J. M. Rowell, Phys. Rev. Letters **14**, 108 (1965).
[j] Per vanadium atom rather than per molecule.
[k] J. E. Kunzler, J. P. Maita, H. J. Levinstein, and E. J. Ryder, Phys. Rev. **143**, 390 (1966).
[l] Bernard Mozer (private communication).

governed by the electronic density of states, being given by $\lambda = N(0)V_{\rm ph}$, with $V_{\rm ph}$ reasonably constant. The coupling-constant variation is certainly correlated with the density-of-states variation, but only because the high-density-of-states materials are elastically softer. We have at present no theoretical explanation of this fact; we have only the empirical observation for these five bcc transition metals.

B. Theory for the Simple Metals

For the polyvalent metals (e.g., Al, In, Pb), the pseudopotential theory[27–29] enables one to calculate all the properties of the metal from a knowledge of the electron-ion pseudopotential. One can calculate the Fermi surface, the electron-phonon matrix elements, and the phonon frequencies. We do not intend to perform detailed calculations here, but rather we will discuss how the coupling constant depends on the pseudopotential, and will obtain some rather simple results.

Within the pseudopotential model, the Hamiltonian of the metal is the sum of (1) the kinetic energy of the electrons, (2) the Coulomb interaction between electrons, (3) the kinetic energy of the bare ions, (4) the Coulomb interaction between ions, and (5) the bare electron-ion interaction given by the pseudopotential $V(R_i - r_e)$. This bare atomic pseudopotential is screened by the conduction electrons, and in momentum space the screened potential is just v_q/ϵ_q, where v_q is the Fourier transform of the bare pseudopotential, and ϵ_q is the dielectric constant. With the atoms located on the lattice sites, the crystal potential is just the sum over lattice sites of this screened potential, and the Fermi surface is determined by the values of v_q/ϵ_q at the reciprocal lattice vectors. For the metals of interest, one finds a Fermi surface distorted slightly from the free-electron sphere, and for this discussion we neglect this distortion and take the wave functions to be plane waves. The electron-phonon matrix elements are now readily calculated from Eqs. (20) and (21). We find

$$g_\nu(p, p') = i(\mathbf{p}-\mathbf{p}')\cdot\epsilon_{p-p',\nu} v_{p-p'}, \tag{34}$$

and, average g^2 over the spherical Fermi surface, we find

$$\langle g^2\rangle = \sum_\nu \int_0^{2k_F} (\epsilon_{q\nu}\cdot q)^2 v_q^2 q\,dq \Big/ \int_0^{2k_F} q\,dq$$

$$= \tfrac{8}{9}k_F^2 E_F^2 \langle v_q^2\rangle, \tag{35}$$

where E_F and k_F are the Fermi energy and wave number, and we have defined a dimensionless average of the pseudopotential squared

$$\langle v_q^2\rangle \equiv \int_0^{2k_F} v_q^2 q^3 dq \Big/ \int_0^{2k_F} v_0^2 q^3 dq. \tag{36}$$

For the free-electron gas, the density of states of one spin per atom is

$$N(0) = 3Z/4E_F, \tag{37}$$

where Z is the valence of the ion. Finally, expressing the average phonon frequency in units of the ionic plasma frequency

$$\Omega_p^2 = 4\pi NZ^2e^2/M, \tag{38}$$

we find an expression for the coupling constant

$$\lambda = N(0)\langle g^2\rangle/M\langle\omega^2\rangle$$

$$= \tfrac{1}{2}\pi \frac{E_F}{k_F e^2} \frac{\langle v_q^2\rangle}{(\langle\omega^2\rangle/\Omega_p^2)}. \tag{39}$$

The factor E_F/k_Fe^2 is just $0.96/r_s$, where r_s is the radius in atomic units of a sphere containing one electron. We find a simple expression for the electron-phonon coupling constant for a nearly-free-electron metal, involving a dimensionless average of the pseudopotential and a dimensionless phonon frequency:

$$\lambda = \frac{1.51}{r_s} \frac{\langle v_q^2\rangle}{(\langle\omega^2\rangle/\Omega_p^2)}. \tag{40}$$

For lead, the tunneling experiments[9] yield the values $\langle\omega^2\rangle/\Omega_p^2 = 0.02$ and $\langle v_q^2\rangle = 0.04$.

Within the pseudopotential model, the phonon frequencies are also determined by the pseudopotential. One starts with a calculation of the phonon frequencies Ω_p of the bare ions and then subtracts the electronic contribution $E_{\rm bs}^2$, which is proportional to $v_q^2(1-1/\epsilon_q)$:

$$\omega_q^2 = \Omega_q^2 - E_{\rm el}^2. \tag{41}$$

The point that we wish to make here is that for the polyvalent metals, there is a large cancellation between the ionic term Ω_p^2 and the electronic term $E_{\rm el}^2$ so that the observed phonon frequencies are extremely sensitive to small changes in $E_{\rm el}^2$ or in the pseudopotential (for lead, the observed ω_q^2 are about $\frac{1}{10}$ of the ionic term Ω_p^2 at the zone boundary). The important dependence of the coupling constant λ upon the pseudopotential arises from the $\langle\omega^2\rangle$ term in the denominator of Eq. (40), rather than from the $\langle v_q^2\rangle$ in the numerator. Thus, for the polyvalent metals, the pseudopotential theory predicts that the coupling constant varies inversely with the (dimensionless) phonon frequency squared:

$$\lambda \cong C/(\langle\omega^2\rangle/\Omega_p^2), \tag{42}$$

[27] J. C. Phillips and L. Kleiniman, Phys. Rev. 116, 287 (1959).
[28] B. J. Austin, V. Heine, and L. J. Sham, Phys. Rev. 127, 276 (1962).
[29] W. A. Harrison, Phys. Rev. 126, 497 (1962); *Pseudopotentials in the Theory of Metals* (W. A. Benjamin, Inc., New York, 1966).

or, more approximately,

$$\lambda \approx C'/M\langle\omega^2\rangle. \tag{43}$$

From Table VII we see that $C'=N(0)\langle\mathcal{I}^2\rangle$ is constant within experimental accuracy for Al, In, and Pb.

To conclude this section, we (1) observe empirically that for a given class (bcc) of transition metals the coupling constant is equal to a constant divided by the ionic mass times the average phonon frequency squared, and (2) show theoretically for the polyvalent metals that this should be the case.

VI. MAXIMUM T_c

For a number of years the highest observed superconducting transition temperature has been 18°K,[30] the "Matthias limit." There has been a great interest, possibly for technological reasons, in the search for higher T_c materials. Recently Matthias *et al.*[31] have found superconductivity at 20°K in a solid solution of Nb_3Al and Nb_3Ge. In that paper the authors state that "there is no theory whatsoever for high transition temperatures of a superconductor." In this section we discuss an upper limit for the transition temperature of a given class of materials.

The strong-coupled theory of superconductivity will predict accurately the transition temperature of a metal from its fundamental properties. The difficulty in trying to predict a maximum T_c is that one does not have an accurate theory of metals from which to calculate the band structure, the phonon spectrum, etc. We can, however, make use of the observation of the preceding section that, within a given class of materials, the coupling constant depends mainly on the phonon frequencies. Given the freedom to adjust the phonon spectrum and therefore the coupling constant, say, by alloying, we show here that T_c has a maximum value.

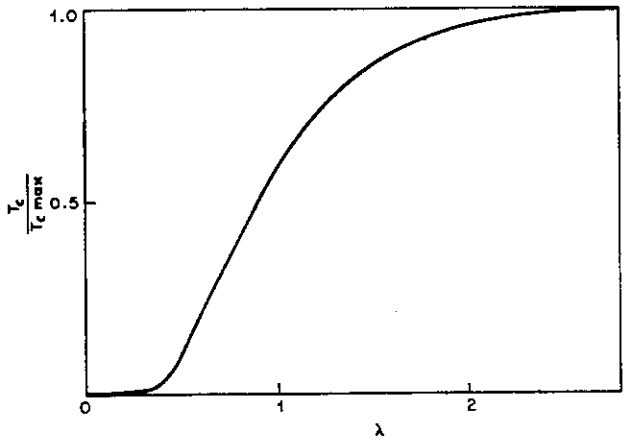

FIG. 11. The superconducting transition temperature according to Eq. (18) with $\mu^*=0.13$, assuming that the coupling constant obeys Eq. (45). Given the transition temperature and coupling constant for a material, the maximum T_c expected for similar materials can be found from this graph.

TABLE VIII. The predicted maximum superconducting transition temperature for four classes of materials found from the observed T_c and λ and Fig. 11, together with the observed maximum T_c.

Metal	T_c (°K)	λ	T_c^{max} (°K)	Observed maximum T_c	Material
Pb	7.2	1.3	9.2	8.8	Pb–Bi
Nb	9.2	0.82	22	10.8	Zr–Nb
V_3Si	17	0.82	40		
Nb_3Sn			28	20	Nb_3Al–Nb_3Ge

Now, using the observation of Sec. V, we write for the coupling constant

$$\lambda = C/M\langle\omega^2\rangle, \tag{45}$$

where C is fixed for a given class of materials, e.g., for the bcc alloys in the neighborhood of Nb. We have

$$T_c = \langle\omega\rangle \exp[-M\langle\omega^2\rangle/C-1], \tag{46}$$

which takes on its maximum value as a function of $\langle\omega\rangle$ for $\langle\omega\rangle=(C/2M)^{1/2}$, and

$$T_c^{max} = (C/2M)^{1/2}e^{-3/2}. \tag{47}$$

What is happening here is that we increase the coupling constant to maximize the exponential factor in Eq. (44) by decreasing the average phonon frequency. But the average phonon frequency premultiplies the exponential, and the product is maximized for $\lambda=2$. It is useful to express T_c/T_c^{max} as a function of λ:

$$T_c/T_c^{max} = (2/\lambda)^{1/2}e^{(1/2-1/\lambda)}.$$

This expression has a broad maximum at $\lambda=2$ and falls off sharply for $\lambda<1$. In Fig. 11, we show T_c/T_c^{max} calculated from the accurate expression for T_c [Eq. (19)] rather than from Eq. (44), and taking $\mu^*=0.13$. Given the T_c and λ for a given material, we can find the maximum T_c for a class of "similar" materials from Fig. 11. The theoretical maximum T_c (Table VIII) for Pb-like materials, that is, for the lead-based alloys, is 9.2°K, and there is in fact a Pb–Bi alloy with $T_c=$

[30] T. H. Geballe, B. T. Matthias, J. P. Remeika, A. M. Clogston, V. B. Compton, J. P. Maita, and H. J. Williams, Physics 2, 293 (1966).
[31] B. T. Matthias, T. H. Geballe, L. D. Loninotti, E. Corenzwit, G. W. Hull, R. H. Willens, and J. P. Maita (to be published).

8.8°K.[32] For Nb-like materials, the maximum observed T_c is about half the theoretical maximum. The value of $T_c^{\max}$ for Nb_3Sn was found by scaling the $T_c^{\max}$ for V_3Si with the square root of the mass ratio.

There are a number of refinements of the theory of $T_c^{\max}$ which should be attempted. The most important one is to test the relationship [Eq. (45)] between the coupling constant and the phonon frequencies for a wider range of materials and also, of course, to attempt to understand this result theoretically for the bcc transition metals. We should note that we have extrapolated the theoretical formula [Eq. (18)] for T_c versus λ, which was derived for $\lambda \lesssim 1$, to larger values of λ. The errors are probably not serious, but the calculations should be carried out for the extreme strong-coupled case. We have assumed that the average phonon frequency can be decreased indefinitely by (for the pseudopotential model) cranking up the pseudopotential. Of course, this is not the case. We are likely to drive some phonon mode unstable, so that the metal prefers a different crystal lattice, before the average phonon frequency is decreased very far. This would set an upper limit on the coupling constant that one could obtain experimentally and provide a stronger upper bound on T_c (a lattice instability of this nature has been observed for V_3Si).[33,34] The fcc Tl–Pb–Bi alloys are an interesting case to study experimentally in this respect, since the coupling constant is already large for lead and apparently increases with bismuth concentration.

VII. CONCLUSIONS

The central result of this paper is Eq. (18), which relates the superconducting transition temperature to the electron-phonon and Coulomb coupling constants according to the strong-coupled theory of superconductivity. This theory is believed to be accurate for real metals to lowest order in an expansion parameter $\hbar\omega_{\rm ph}/E_F \sim 10^{-2}$–$10^{-3}$. The equations were originally derived for the Frohlich Hamiltonian, but recent studies[35–37,9] of the Coulomb interaction indicate that the only effect of the Coulomb interactions is to renormalize the energy bands and the electron-phonon matrix elements, and that the structure of the self-energy equations used here is correct. Band-structure effects are properly included in the definition of λ. We have neglected the anisotropy of the energy gap, but this introduces only a small error in T_c. The effects of persistent spin fluctuations, which are important for the nearly ferromagnetic case, are believed to be unimportant for the metals considered here. These effects could probably be included within the present formalism by choosing a somewhat larger Coulomb term μ^*. We have made one special assumption by using the phonon density of states for niobium. This introduces important errors only for the strong-coupled ($\lambda > 1$) superconductor with a wildly different phonon spectrum. We note that the strong-coupled theory has received strong experimental support from the analysis of the tunneling experiments on lead which probes the detailed structure of the self-energy equations. We regard Eq. (18) as just the numerical consequence of the established and verified theory of superconductivity. We have made no attempt to verify the theory of superconductivity in this paper, but rather have used that theory to examine the electron-phonon interaction in those metals which are superconducting. Equation (18) proves to be very useful in estimating the electron-phonon interaction strength and in stripping away the "phonon enhancement" of the specific heat and cyclotron mass to reveal the "band-structure" values. We have examined the variation of the coupling constant over limited portions of the periodic table and have found a surprising result—namely, that the coupling constant depends mainly on the phonon frequencies and is insensitive to large variations in the electronic properties, e.g., the band-structure density of states. This observation has been used to predict a maximum transition temperature for a given class of materials.

ACKNOWLEDGMENTS

The author would like to thank T. H. Geballe for stimulating discussions, K. Andres and E. Bucher for helpful discussions of the experimental data and for communication of their results prior to publication, and L. F. Matthies for discussions of his beautiful band-structure calculations and for permission to use Fig. 10. The author has greatly benefited from discussions of the theory of superconductivity with a number of colleagues, notably P. W. Anderson, A. M. Clogston, J. W. Garland, D. J. Scalapino, J. R. Schrieffer, and J. C. Swihart.

[32] B. W. Roberts, *Progress in Cryogenics* (Heywood and Co., Ltd., London, 1964).
[33] B. W. Batterman and C. S. Barrett, Phys. Rev. Letters **13**, 390 (1964).
[34] L. Testardi, T. B. Bateman, W. A. Reed, and V. G. Chirba, Phys. Rev. Letters **15**, 537 (1965).
[35] E. G. Batyev and V. L. Pokrovskii, Zh. Eksperim. i Teor. Fiz. **46**, 262 (1963) [English transl.: Soviet Phys.—JETP **19**, 181 (1964)].
[36] V. Heine, P. Nozieres, and J. W. Wilkins, Phil. Mag. **13**, 741 (1966).
[37] R. E. Prange and S. Sachs, Phys. Rev. **158**, 672 (1967).